Thermoelectric performance using counter-flowing thermal fluids

Baiyi Lu [a], **Xiangning Meng** [a, *], **Yue Tian** [a], **Miaoyong Zhu** [a], **Ryosuke O. Suzuki** [b]

[a] *School of Metallurgy, Northeastern University, Shenyang 110819, China*

[b] *Faculty of Engineering, Hokkaido University, Sapporo 060-8628, Japan*

[*] Corresponding author. Tel.: +86 24 83671706; fax: +86 24 23906316.

E-mails address: mengxn@smm.neu.edu.cn (X. Meng)

Abstract

Counter-flowing thermal fluids are conducive to generate a homogeneous temperature difference on thermoelectric (TE) generator. This study allowed the hot and cold fluids of having constant inlet temperature to flow in the opposite, and examined TE performance of module at different flow rates. The results show that TE performance gradually increases with flow rate in the initial stage of fluid flow, and reaches a transient peak value after the module surfaces are completely covered by thermal fluids, and then tends to be stable. High flow rate leads to larger performance and reduces the time of achieving them. Effect of flow rate on stable performance is slightly more than that of inlet temperature of thermal fluids, which makes regulating the flow rate to be a feasible way to harvest more heat for TE conversion. Module features present a specific trend and provide the supports for the benefit of counter-flowing thermal fluids.

Key words

Thermoelectric generation; Thermoelectric performance; Counter-flowing thermal fluids; Flow rate; Finite-element analysis

1. Introduction

Thermoelectric (TE) conversion is bound to be a promising technology for the acquisition and utilization of renewable and recycled resources [1-4], such as inexhaustible solar energy and industrial waste heat, because the thermal feeding can be directly converted into electricity at a junction of two different materials by using a TE generator (TEG) based on the Seebeck effect [5, 6], and TEGs can be operated reliably in an isolated place without noise and pollution, and the chemical reactions or mechanical moving parts are no longer needed [7, 8]. In essence, TE generation requires a sufficient temperature difference, ΔT, between hot and cold surfaces of TEGs to induce an electromotive force (EMF), and a high ΔT leads to a high EMF, which is attributed to EMF is the sum of the product of the relative Seebeck coefficient and the temperature difference for all p-type and n-type TE elements connected in serial [9], moreover, we had clarified that the homogeneous heat flux throughout a TEG is indispensable to enhance TE performance that is due to the geometry-dependent thermal diffusion becomes uniform [10, 11]. Thus as a result, a pair of counter-flowing hot and cold fluids, as shown in **Figure 1 (a)**, should give rise to a better TE conversion on module, where a high ΔT can be facilitated by the hot fluid, and a homogeneous heat flux can be obtained when the hot fluid is cooled and the cold fluid is heated at the same time by exchanging the heat through the conduction of solid TE module in the process of the thermal fluids flow in the opposite, as depicted in **Figure 1 (b)**.

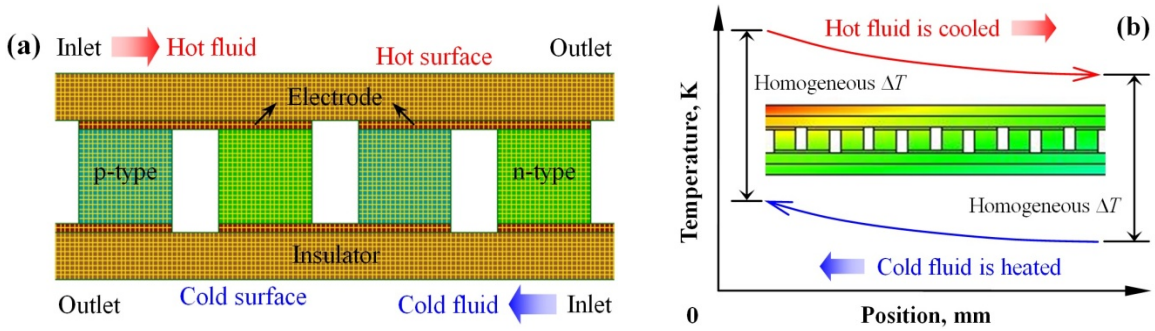

Figure 1 TE module using counter-flowing thermal fluids:
(a) 3D physical model and **(b)** temperature difference formation.

The benefits of counter-flowing fluids are widely recognized, but the thermoelectric effects by their flows have been less studied. Our previous work [12] investigated the influence of temperature difference between a pair of counter-flowing hot and cold fluids on the performance of a TE module, including voltage and electric current, as well as output power, input heat and conversion efficiency, and indicated that the transient performance tends to be stable over a period of time after TE module surfaces are completely covered by the thermal fluids, where this delay time is consistent for the different inlet temperature of hot fluid when the inlet temperature of cold fluid and the flow rate of fluids are fixed, and the stable performance increases with the inlet temperature of hot fluid, and that the counter-flowing fluids can simultaneously produce a homogeneous distribution for electric charges and heat flux throughout the entire module composed of the conventional cube-shaped TE elements. This study continued to model a three-dimension (3D) TE module whose surfaces are covered by the counter-flowing hot and cold fluids, and conducted a numerical simulation using finite-volume method in a commercial software environment, Fluent, to clarify the change of module performance with the flow rate of thermal fluids, where fluid dynamics and TE conversion are carried out synchronously, and then the effects of temperature difference and flow rate on TE performance are compared, which illuminates that the regulation of flow rate should be more effective in improving performance of TE module. The uniform thermal diffusion brings about a homogeneous distribution of pressure and enthalpy inside TE module and exhibit a specific trend with flow rate.

2. Finite-Element Solution

2.1. 3D Meshed Model

Figure 2 showed a cross-section design of the two cuboid-shaped channels on TE module in order to allow the thermal fluids flow in them and then cover the hot and cold surfaces, where the module surfaces are regarded as the channel floors, and each channel contains two walls and a ceiling to act as the borders of fluid flow. Counter-flowing hot and cold fluids flow into channel via the inlet and exit through the outlet, respectively, and are directly in contact with TE module to provide the required temperature difference for TE conversion. 3D physical model is divided into two computational domains, one is used to calculate the pure flow behavior of thermal fluids, including two channels, and the other is the entire module to implement the simulation on TE process consisting of heat conduction and electric charge transport, and the heat supply from the counter-flowing fluids is considered as the thermal boundary condition. Two computational domains are meshed three-dimensionally by the same size, 0.05 mm, using map mesh method to achieve the sufficient convergence and precision for the repeated finite-element iterations. For simplification, the following assumptions are made in formulating 3D physical model: 1) TE module is adiabatic to the outside, 2) a perfect tight bonding exists among all the component parts of module, 3) the temperature-dependent properties of solid module materials are

ignored because no obvious performance change was found in a narrow temperature range [13], 4) the thermal fluids flow in the form of uniform laminar at a fixed flow rate, and the fluid compression and turbulent buoyancy in channel are neglected, thereby no changes in the pressure and volume for them, and 5) the hot and cold fluids are considered as the oil and water, respectively, and the physical properties of high-temperature oil are close to those of water at ambient temperature, so that ensure the one-way flow and the heat transfer of fluids are in a similar situation. TE module is constituted by 18 pairs of cube-shaped elements of p-type and n-type, which are connected together in series using electrode plates, and sandwiched between the insulator layers. The geometric dimensions of 3D physical model as well as the properties of thermal fluids and solid materials are listed in **Table 1**, **Table 2** and **Table 3**, respectively.

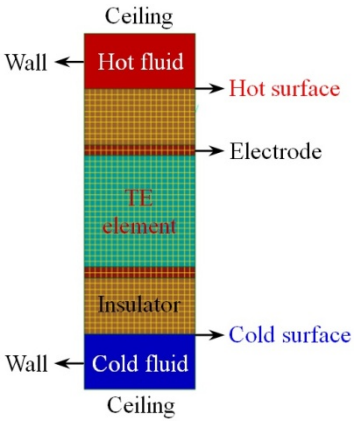

Figure 2 Cross-section design of TE module for finite-element analysis.

Table 1 Geometric dimensions of 3D physical model.

TE elements	Electrode plate		Insulator layer		Channels	
Edge length (mm)	Thickness (mm)	Width (mm)	Thickness (mm)	Width (mm)	Wall (mm)	Ceiling (mm)
1.0	0.1	1.0	0.5	1.0	0.5	1.0

Table 2 Physical properties of thermal fluids at ambient temperature.

Density ($kg \cdot m^{-3}$)	Specific heat ($kJ \cdot kg^{-1} \cdot K^{-1}$)	Viscosity ($10^{-5} \cdot Pa \cdot s$)	Thermal conductivity ($W \cdot m^{-1} \cdot K^{-1}$)
1000	4.18	100	0.6

Table 3 Thermal and electric properties of solid materials.

Materials		Seebeck coefficient ($\mu V \cdot K^{-1}$)	Electric resistivity ($10^{-6} \cdot \Omega \cdot m$)	Thermal conductivity ($W \cdot m^{-1} \cdot K^{-1}$)
Bi_2Te_3	(p-type)	190	5.5	2.06
Bi_2Te_3	(n-type)	210	10.0	2.02
Cu	(electrode)	1.83	0.0155	398
Al_2O_3	(insulator)			36

2.2. Governing Equations

Uniform laminar flow causes the channel to be filled with the thermal fluids, and the continuity equation

describing the mass conservation of incompressible fluids from inlet to outlet is express as:

$$\nabla \cdot v_x = 0 \tag{1}$$

where v_x is the fixed flow rate of thermal fluids in one-way direction.

Thermal fluids in laminar flow follow the Euler equation [14] because the pressure drop in channel is only affected by the gravity of fluids, and the motion equation is expressed as:

$$f - \frac{1}{\rho}\nabla p = \frac{\partial v_x}{\partial t} \tag{2}$$

where ρ is the density of thermal fluids, f is the mass force caused by the gravity, and p is the pressure in channel. Heat of thermal fluids is fed to TE module so as to form a temperature difference between the hot and cold surfaces, and then results in a TE conversion. This study concurrently conducted the iterative calculations of internal heat transfer and electric charge transportation for microscopic finite-element volumes because the macroscopic heat diffusion analysis is unable to illuminate the distributions of temperature and current density inside TE module. The steady-state heat conduction in each control volume is solved by the energy conservation, including the Joule heat generated by the current and the heating or cooling caused by the Thomson effect, and the differential equation that follows the Fourier law is expressed as:

$$\nabla \cdot (\lambda \Delta T) = T\boldsymbol{J} \cdot \nabla S - \sigma|\boldsymbol{J}|^2 \tag{3}$$

where λ, σ, and S denote the thermal conductivity, the electric resistivity, and the relative Seebeck coefficient, respectively, and the current density, $\boldsymbol{J}$, is obtained by the electric potential and temperature, expressed as:

$$\sigma\boldsymbol{J} = -\nabla V - S\nabla T \tag{4}$$

where the voltage due to $\sigma\boldsymbol{J}$ is given by the change in the electric potential, ∇V, and the voltage generated from the Seebeck effect, $S\nabla T$, and then the governing equation of TE conversion is derived by applying the electric charge conservation, expressed as:

$$\nabla \cdot (\nabla V + S\nabla T) = 0 \tag{5}$$

Following **Eq. 1** and **Eq. 2**, the calculations of laminar flow are executed on each mesh in the computational domain of channels once the counter-flowing fluids flow into the channel through the inlet, and the macroscopic heat carried by the fluids is transferred to the hot and cold surfaces of TE module to play a role of thermal boundary condition, meanwhile, the numerical simulations are performed in the computational domain of entire module by solving the simultaneous differential equations of **Eq. 3** and **Eq. 5** on the control volumes. By referring to the reported codes [15], our custom-written C program is embedded into the commercial software package, Fluent, and combined with the conventional codes to evaluate the current density using finite-volume method [13, 16].

3. Results and Discussion

3.1. Transient Performance

Initial conditions for TE module are set as: 1) fixed flow rates of uniform laminar of counter-flowing thermal fluids are successively changed to 2 mm·s^{-1}, 4 mm·s^{-1}, 6 mm·s^{-1}, 8 mm·s^{-1}, and 10 mm·s^{-1}, and flow rates of 15 mm·s^{-1} and 20 mm·s^{-1} are also considered to investigate the impact of high flow rates on TE performance, and 2) inlet temperatures of hot and cold fluids are constant at 500 K and 300 K, respectively. Further, the flow time of thermal fluids is maintained at least 55 s in order to satisfy the requirement of the fluid with lowest flow rate can completely the module surface as well as to stabilize TE conversion as far as possible.

Transient performance of module is calculated by using finite-element analysis on 3D meshed model, including voltage, electric current and output power from the fluids flow into the channel inlet until a steady trend, as shown in **Figure 3**. The voltage and current present a direction opposite to the follow-up voltage and current in the initial stage of about 1.0 s. This is because in this stage the local temperature difference produced the electromotive force using the p-type and n-type elements near the channel inlets, which is based on the Seebeck effect, and the electric current was also naturally generated on the entire module. However, the others p-n pairs are bound to concurrently consume this electric current to form a reverse temperature gradient through the Peltier effect, and then cause the short-lived voltage and electric current in a converse direction. Subsequently, the voltage and current are gradually increased along with the thermal fluids covering the module surfaces, as shown in **Figure 3 (a)** and **(b)**. The performance failed to achieve a stable value in their respective theoretical time that the hot and cold surfaces are completely covered by the thermal fluids, such as 26.75 s for flow rate 2 mm·s^{-1} and 5.35 s for flow rate 10 mm·s^{-1} and so on. High flow rate of fluids increases the voltage and current quickly, also makes them to reach the stable value as soon as possible, and higher flow rate brings higher stable performance. The performance caused by the high flow rates of 6 mm·s^{-1}, 8 mm·s^{-1}, and 10 mm·s^{-1} tends to be stable after a peak value, which is indicated by triangle symbols, while low flow rate leads to a steady rise in performance without causing a peak value. For example, the peak values of voltage and current for flow rate 10 mm·s^{-1} appear in about 10.5 s after the beginning of fluid flow, and those of for flow rate of 2 mm·s^{-1} and 4 mm·s^{-1} continues to improve smoothly. **Figure 3 (c)** showed that the output power of module presents a trend from decline to rise due to the short-lived voltage and electric current in the initial stage, and its succedent change is similar to that of voltage and current. Further, a sustained increase in flow rate results in a sharp enhancement in performance, and the time to reach the peak values is shortened and the stable values are significantly improved. For example, the comparison of output power at flow rates of 10 mm·s^{-1}, 15 mm·s^{-1} and 20 mm·s^{-1} is shown in **Figure 3 (d)**, where their peak output power are 128.9 μW, 211.8 μW and 284.6 μW, and the time of obtaining them are 11.0 s, 8.5 s and 7.5 s, respectively.

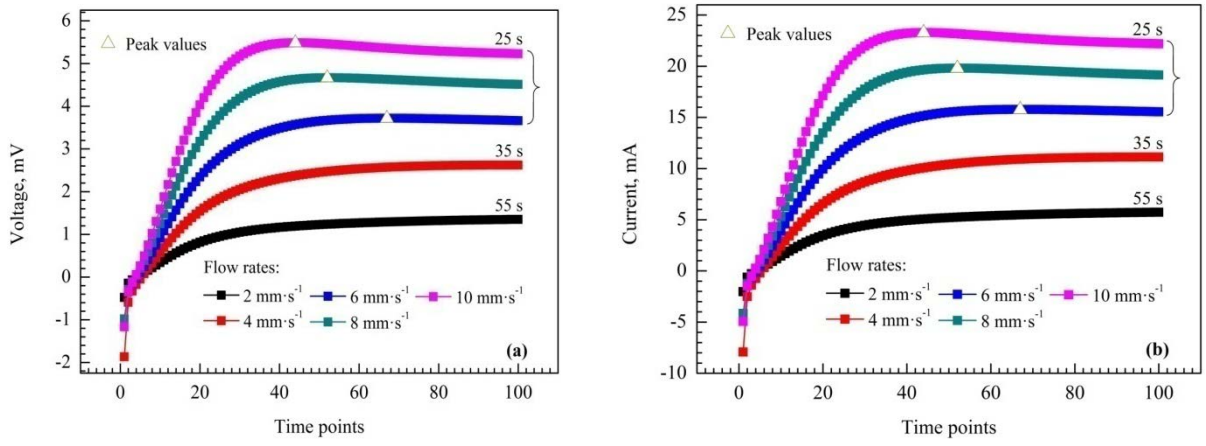

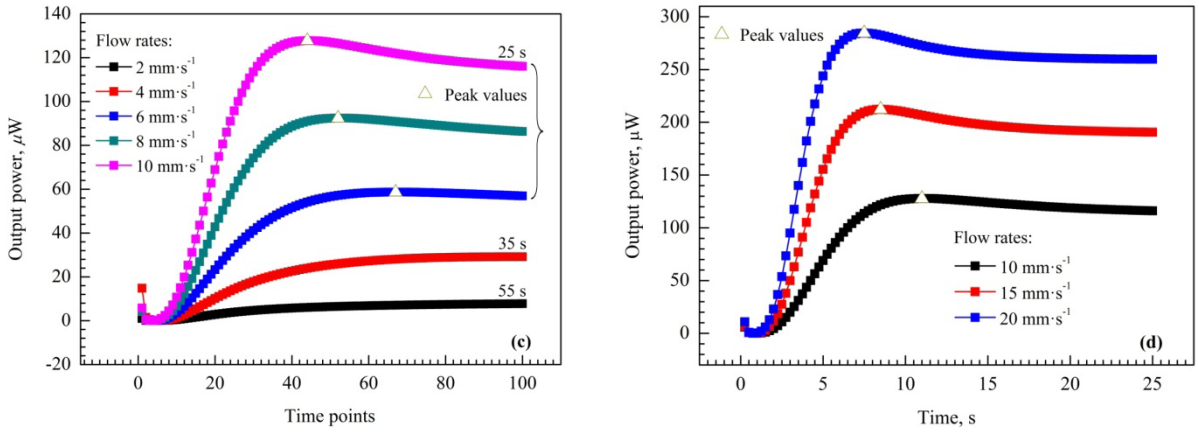

Figure 3 Transient performance of TE module:
(a) voltage, **(b)** current, and **(c)** output power at low flow rates, as well as **(d)** output power at high flow rates.

3.2. Performance Comparison

Based on the same physical model, we have investigated the transient performances at different inlet temperature of 400 K, 450 K, 500 K, 550 K and 600 K for hot fluid by using a flow rate of 5 mm·s^{-1} and a constant inlet temperature 300 K for cold fluid, and confirmed [12] that the delay time of the initial stage for reverse voltage and current is consistent for all inlet temperature of hot fluid when the inlet temperature of cold fluid and the flow rate of counter-flows are fixed, and the transient performance is steadily rising to a stable value and no peak value appeared. These results are obviously different from those effects of flow rate on the performance, and then stimulated a necessity to compare the stable performances caused by the change of inlet temperature of hot fluid and flow rate of counter-flowing fluids, so as to distinguish the influence degree of them on TE performance improvement.

Stable performance is naturally increased with inlet temperature and flow rate, as shown in **Figure 4**. Inlet temperature has a linear effect on the voltage and electric current because the temperature difference of module changes regularly when a fixed flow rate of 5 mm·s^{-1} is used as well as the electromotive force is the sum of the multiplication of the relative Seebeck coefficient and the temperature difference for all elements connected in serial. However, the temperature difference does not strictly change with flow rate, so that the performance presents a non-linear trend, as shown in **Figure 4 (a)** and **(b)**, and the voltage and electric current generated by the low flow rate of 2 mm·s^{-1} are still slightly lower than those of using fixed rate of 5 mm·s^{-1} and inlet temperature of 400 K, although with a high inlet temperature of 500 K. Further, the voltage and current using constant inlet temperature correspondingly exceeds those of using fixed flow rates, especially the performance is significantly enhanced when the flow rate is improved to 15 mm·s^{-1} and 20 mm·s^{-1}. Output power for two different conditions is calculated in **Figure 4 (c)**, and presents a similar trend to voltage and current and is significantly elevated at high rates. Hence, we can draw a preliminary conclusion that the influence of flow rate of counter-flowing fluids on the stable performance is slightly more significant than that of inlet temperature of thermal fluids, which allows the regulation of flow rate to be an effectual way for TE performance improvement because the flow rate control should be more viable than a high temperature maintenance. **Figure 4 (d)** showed that more energy is carried to TE module by increasing flow rate and inlet temperature. Linear increase in inlet temperature leads to a linear increase of input heat, while flow rate does not in this case, and its increase is relatively smooth at high flow rate. Conversion efficiency of TE module is determined by the ratio of output power to input heat, as shown in **Figure 4 (e)**, where high inlet temperature and flow rate can bring a high conversion efficiency for TE generation, and that the deserved concern is the efficiency enhancement at high

flow rates of 15 mm·s^{-1} and 20 mm·s^{-1}, which attributed to the corresponding high output power. So, another preliminary conclusion can be drawn that the utilization of counter-flowing thermal fluids with high flow rate is a promising approach to harvest more heat for TE conversion.

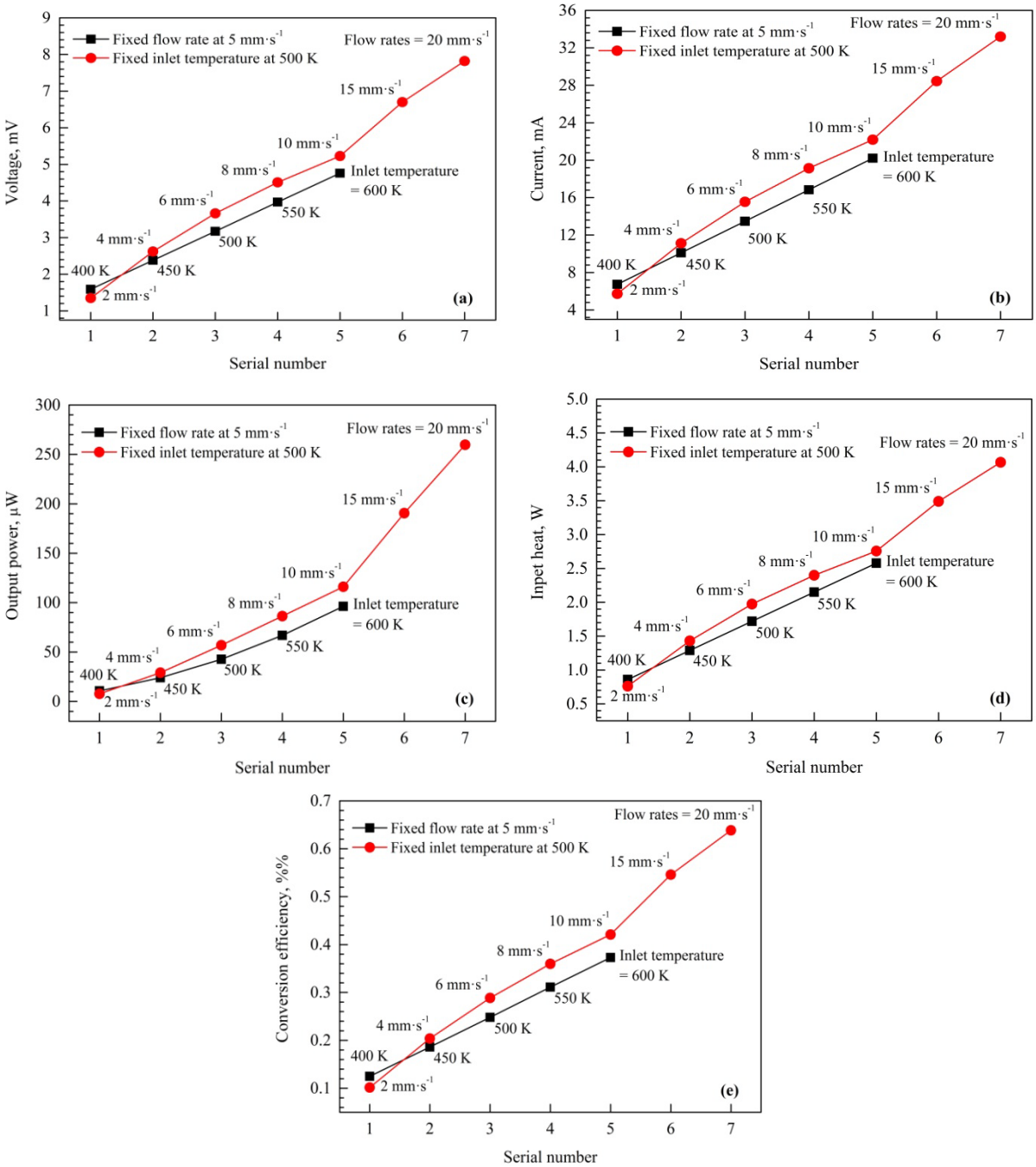

Figure 4 Stable performance comparison of TE module:
(a) voltage, **(b)** current, **(c)** output power, **(d)** input heat, and **(e)** conversion efficiency.

3.3. Module Features

The specific features on TE module is induced by using the counter-flowing fluids as the thermal boundary and helps to clarify the influence of counter-flowing fluids on TE performance. A case of temperature distribution of module is given in **Figure 5**. The hot and cold fluids in counter-flowing do form a homogeneous temperature

difference on 3D physical model, while the temperature of thermal fluids and the temperature drop from inlet to outlet of channel are significantly affected by the difference of flow rates, where high flow rate of 10 mm·s^{-1} brings about a rapid increase of overall temperature of module compared to low flow rate of 2 mm·s^{-1}.

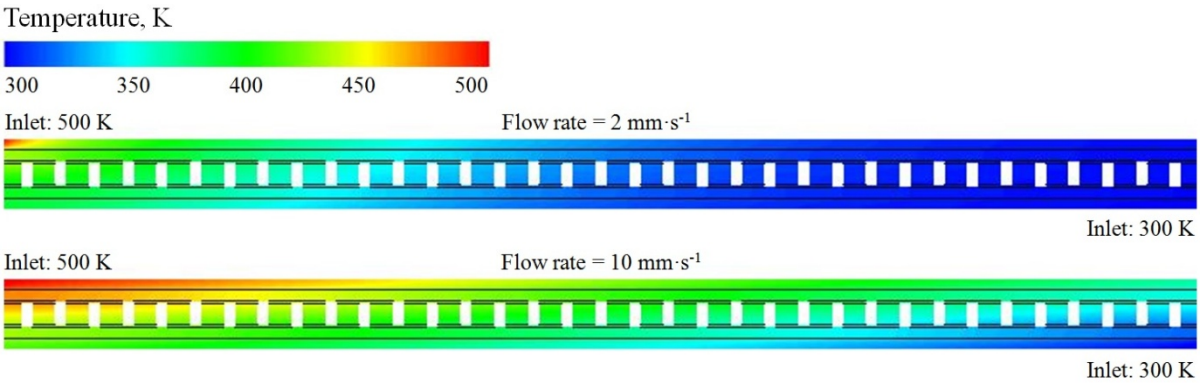

Figure 5 Distribution of temperature on TE module.

The outlet temperature of hot fluid is almost linearly increased with flow rate from 302 K at 2 mm·s^{-1} to 406 K at 10 mm·s^{-1} due to the combined action of cold fluid cooling and rapid carrying of heat on flow path, as shown in **Figure 6 (a)**, while the outlet temperature of cold fluid changes gently because it largely depends on the inlet temperature of hot fluid of 500 K. The outlet temperature of cold fluid increases in the rate range from 2 mm·s^{-1} to 10 mm·s^{-1} and decreases in the rate range from 10 mm·s^{-1} to 20 mm·s^{-1}, indicating that at least the local temperature difference is enlarged when the flow rate of thermal fluids exceeds a certain value, such as 10 mm·s^{-1} in the present study, thereby enhancing the Seebeck effect, which also explains the improvement in TE performance at high flow rate. Meanwhile, the temperature drop in channel can be obtained in **Figure 6 (b)**, where the drop in hot fluid strictly decreases with flow rate, and the drop in cold fluid certainly decided by the range of flow rate, increases at low rate and decreases at high rate, respectively. Interestingly, the temperature drop tends to be consistent for the hot and cold fluids at flow rates of 15 mm·s^{-1} and 20 mm·s^{-1}, indicating that the high flow rate is favorable to form a homogeneous temperature difference throughout the entire module because the uniform temperature drop inevitably leads to the similar temperature difference between the hot and cold surfaces, which again proves that the high flow rate is beneficial to TE performance.

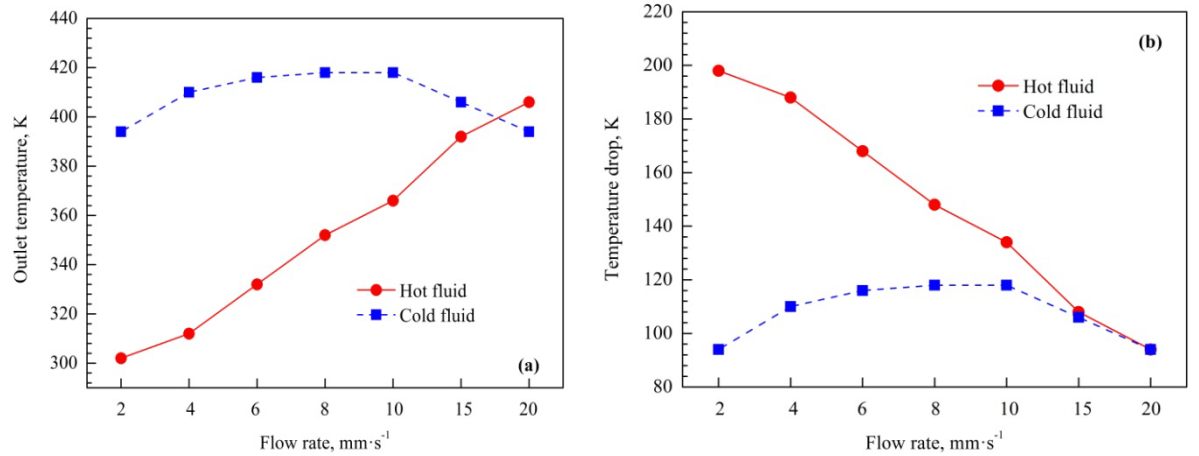

Figure 6 Temperature of thermal fluids in channel:
(a) outlet temperature and **(b)** temperature drop from inlet to outlet.

Pressure of thermal fluids in laminar flow exhibits a downward trend from inlet to outlet of channel, and **Figure 7** showed a 3D case in which the pressure of hot fluid is significantly higher than that of cold fluid because of their own gravity, and high flow rate of 10 mm·s^{-1} causes a quick enhancement of overall pressure in channel compared to low flow rate of 2 mm·s^{-1}. High flow rate causes the channel inlet to be matched with a high pressure, as shown in **Figure 8 (a)**, and only a valley pressure occurs at flow rate of 8 mm·s^{-1} for the hot fluid. The valley pressure may be due to the low head loss and less pressure compensation in channel, which is decided by the hydraulic dimensions and characteristics, and will be reported separately after an honest study. However, the pressure drop between the inlet and outlet of channel strictly increases with flow rate, as shown in **Figure 8 (b)**, and the drop trend of two fluids is similar, where the pressure drop is almost equal at low flow rates from 2 mm·s^{-1} to 8 mm·s^{-1}, and is only slightly differentiated at high flow rates from 10 mm·s^{-1} to 20 mm·s^{-1}, as a consequence, the uniform pressure drop is advantageous to implement TE generation by using counter-flowing fluids as thermal sources.

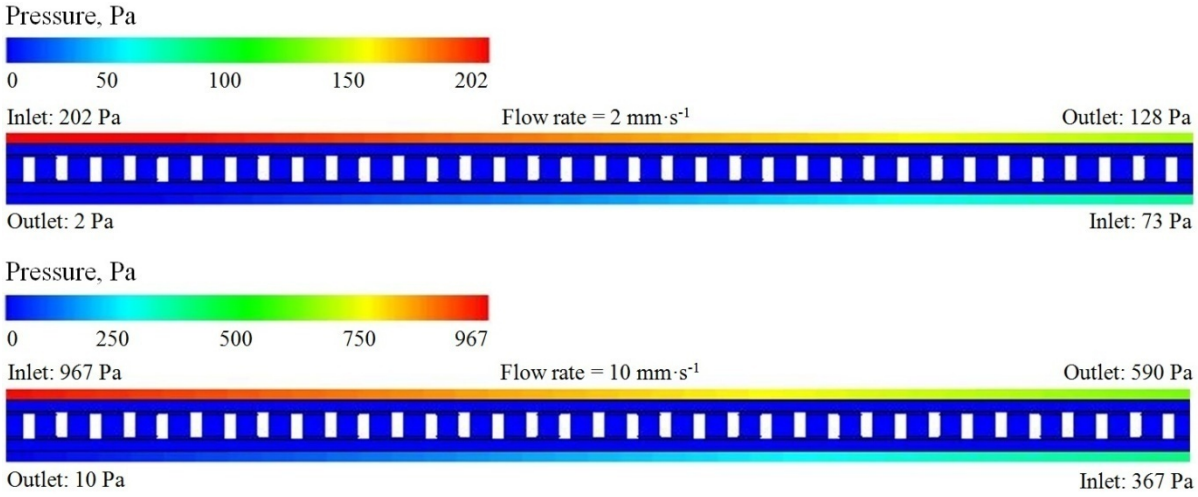

Figure 7 Pressure in channels of TE module.

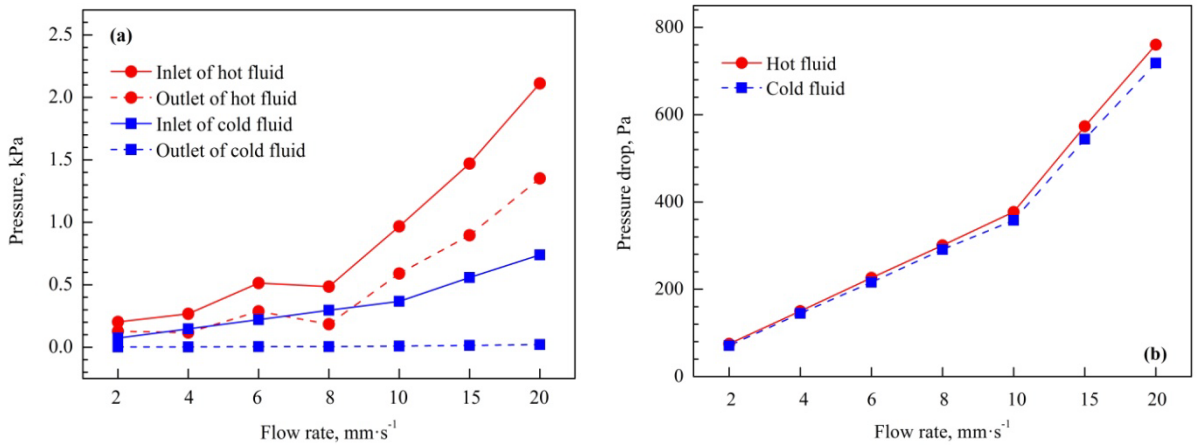

Figure 8 Pressure of thermal fluids in channel:
(a) inlet and outlet pressure and **(b)** pressure drop from inlet to outlet.

High temperature surely leads to more energy change, resulting in maximum and minimum enthalpies present at channel inlets of hot and cold fluids, as shown in **Figure 9**. High flow rate of 10 mm·s^{-1} can speedily make TE module in a high enthalpy compared to low flow rate of 2 mm·s^{-1}. For low flow rate of 2 mm·s^{-1}, the heat carried

by the thermal fluids is insufficient to fully complement the internal energy of TE module and then makes TE module endothermic, and the maximum and minimum enthalpies are about 847.3 kJ·kg^{-1} and 3.1 kJ·kg^{-1}, respectively. As the flow rate increases, more heat is transferred to TE module timely, so that the heat exchange between the thermal fluids and TE module is in a dynamic equilibrium, and the maximum and minimum enthalpies remain constant as about 847.8 kJ·kg^{-1} and 7.78 kJ·kg^{-1}, respectively, as shown in **Figure 10**. In theory, a lower flow rate can allow TE module to achieve a state of internal energy saturation, which enables more heat to be used for thermal diffusion and TE conversion on module.

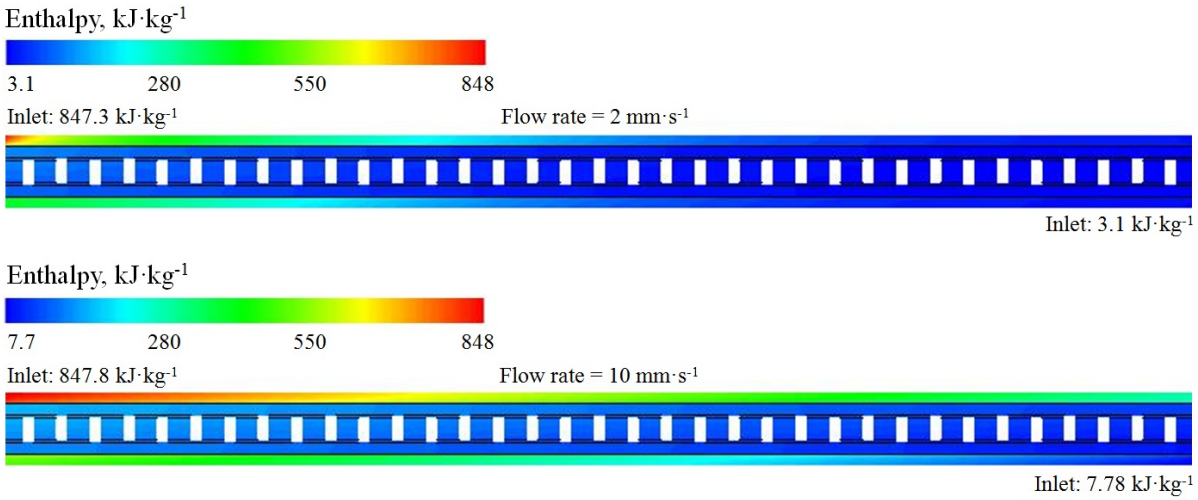

Figure 9 Enthalpy on TE module.

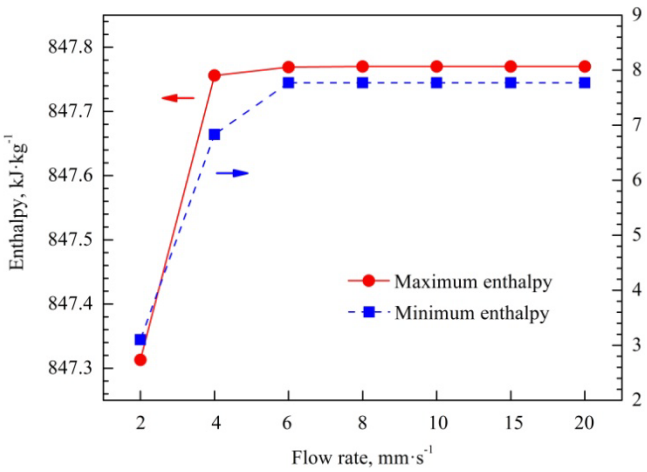

Figure 10 Enthalpy extrema of TE module.

4. Conclusions

Using finite-element simulation, this study examined the influence of flow rate on TE performance under the condition that the counter-flowing fluids are considered as the thermal boundary of a TE module, which can form a homogeneous thermal distribution. Moreover, the module features induced by the counter-flowing thermal fluids are clarified. The results are drawn as follows:

(1) Transient performance tends to be stable over a period of time after the module surfaces are completely covered by the counter-flowing fluids. The delay time is shortened with the flow rate when the inlet temperature of fluids is fixed.

(2) Stable performance can be obtained as soon as possible with high flow rate of thermal fluids and the performance values increase with flow rate. High flow rate leads to high performance for a TE module of using constant inlet temperature of thermal fluids.

(3) Impact of flow rate on stable performance is stronger than that of inlet temperature of thermal fluids. The regulation of flow rate of counter-flowing fluids is an effectual way for TE performance improvement. Utilization of counter-flowing fluids at high flow rate is a promising approach to harvest more heat for TE conversion.

(4) Specific module features indicated that a local temperature difference can be enlarged and a homogeneous temperature difference can be obtained at high flow rate, and uniform pressure drop in channel is advantageous to implement TE generation, as well as a lower flow rate allows TE module to achieve a state of internal energy saturation and enables more heat to be used for thermal diffusion and TE conversion.

Acknowledgements

The authors are grateful to financial supports from National Natural Science Foundation of China (51576034) and Fundamental Research Funds for the Central Universities of China (N162502001).

References

1. Shi X, Chen L. Thermoelectric materials step up. Nat Mater 2016; 15: 691-692.
2. Borset MT, Wilhelmsen O, Kjelstrup S, Burheim OS. Exploring the potential for waste heat recovery during metal casting with thermoelectric generators: on-site experiments and mathematical modeling. Energy 2017; 118: 865-875.
3. Nishibori M, Shin W, Izu N, Itoh T, Matsubara I, Yasuda S, Ohtani S. Robust hydrogen detection system with a thermoelectric hydrogen sensor for hydrogen station application. Int J Hydrogen Energy 2009; 34: 2834-2841.
4. Chiriac R, Racovitza A, Podevin P, Descombes G. On the possibility to reduce CO_2 emissions of heat engines fuelled partially with hydrogen produced by waste heat recovery. Int J Hydrogen Energy 2015; 40: 15856-15863.
5. Snyder GJ, Toberer ES. Complex thermoelectric materials. Nat Mater 2008; 7: 105-114.
6. Molina MG, Juanicó LE, Rinalde GF. Design of innovative power conditioning system for the grid integration of thermoelectric generators. Int J Hydrogen Energy 2012; 37: 10057-10063.
7. Bell LE. Cooling, heating, generating power, and recovering waste heat with thermoelectric systems. Science 2008; 321: 1457-1461.
8. Hwang J, Lin C, Kuo J. Performance analysis of fuel cell thermoelectric cogeneration system with methanol steam reformer. Int J Hydrogen Energy 2014; 39: 14448-14459.
9. Suzuki RO. Mathematic simulation on power generation by roll cake type of thermoelectric double cylinders. J Power Sources 2004; 133: 277-285.
10. Meng X, Suzuki RO. Performance analysis of thermoelectric modules using polyhedron elements. Mater Trans 2015; 56: 1092-1095.
11. Meng X, Suzuki RO. Simulation analysis of tilted polyhedron-shaped thermoelectric elements. J Electron Mater 2015; 44: 1469-1476.
12. Meng X, Lu B, Zhu M, Suzuki RO. Thermoelectric generation using counter-flows of ideal fluids. J Electron Mater 2017; 46: 10.1007/s11664-017-5518-5.
13. Fujisaka T, Sui H, Suzuki RO. Design and numerical evaluation of cascade-type thermoelectric modules. J Electron Mater 2013; 42: 1688-1696.

14. Zhang XZ. Principles of Transfer in Metallurgy. 1st Edition, Metallurgical Industry Press, Beijing, 2005; p.42.
15. Chen M, Rosendahl LA, Condra T. A three-dimensional numerical model of thermoelectric generators in fluid power systems. Int J Heat Mass Transf 2011; 54: 345-355.
16. Meng X, Suzuki RO. Helical configuration for thermoelectric generation. Appl Therm Eng 2016; 99: 352-357.

Figure captions

Figure 1 TE module using counter-flowing thermal fluids: **(a)** 3D physical model and **(b)** temperature difference formation.

Figure 2 Cross-section design of TE module for finite-element analysis.

Figure 3 Transient performance of TE module: **(a)** voltage, **(b)** current, and **(c)** output power at low flow rates, as well as **(d)** output power at high flow rates.

Figure 4 Stable performance comparison of TE module: **(a)** voltage, **(b)** current, **(c)** output power, **(d)** input heat, and **(e)** conversion efficiency.

Figure 5 Distribution of temperature on TE module.

Figure 6 Temperature of thermal fluids in channel: **(a)** outlet temperature and **(b)** temperature drop from inlet to outlet.

Figure 7 Pressure in channels of TE module.

Figure 8 Pressure of thermal fluids in channel: **(a)** inlet and outlet pressure and **(b)** pressure drop from inlet to outlet.

Figure 9 Enthalpy on TE module.

Figure 10 Enthalpy extrema of TE module.

Table captions

Table 1 Geometric dimensions of 3D physical model.

Table 2 Physical properties of thermal fluids at ambient temperature.

Table 3 Thermal and electric properties of solid materials.